Archives of Dermatological Research (2025) 317:352
https://doi.org/10.1007/s00403-025-03866-z

ORIGINAL PAPER

# Therapeutic potential of phloridzin carbomer gel for skin inflammatory healing in atopic dermatitis

Fulu Lv[1,3] · Yanxia Chen[1,3] · Haohui Xie[4] · Manzhi Gao[3] · Ruohong He[3] · WanYing Deng[2] · Weiqiang Chen[1,3]

Received: 7 December 2024 / Revised: 10 January 2025 / Accepted: 18 January 2025


## Abstract

Phloridzin (PL), a natural compound derived from apples, exhibits diverse pharmacological properties including anti-inflammatory, anti-tumor, antioxidant, and anti-aging effects. The present study aimed to evaluate the impact of Phloridzin Carbomer Gel (PL-CG) on skin inflammatory healing in a mouse model of atopic dermatitis (AD). In vitro experiments initially determined the non-toxic concentration range of PL in cells, established a cellular inflammation model by stimulating cells with histamine to ascertain the optimal therapeutic concentration of PL, and subsequently detected decreased mRNA expression levels of relevant inflammatory cytokines, interleukins, through RT-qPCR experiments following PL treatment. For in vivo experiments, an AD mouse model was constructed. Histopathological analysis, along with assessments of epidermal thickness, reduction in scratch counts on the back of mice, and healing rates of inflammatory areas, indicated that PL-CG facilitates epidermal tissue regeneration and wound repair, thereby accelerating skin inflammatory healing. Additionally, PL-CG was subjected to microstructural observation using scanning electron microscopy (SEM), and experiments were conducted to determine its optimal pH value, stability, viscosity, and the influence of different concentrations of carbomer gel on drug release. The study demonstrated that PL-CG possesses anti-inflammatory and antipruritic properties, as well as the ability to promote skin inflammatory healing. Compared to traditional corticosteroids, PL-CG exhibits a higher safety profile and fewer side effects, suggesting broad prospects for its clinical application in the treatment of atopic dermatitis.

**Keywords** Atopic dermatitis; · Anti-inflammatory; · Phloridzin carbomer gel; · Skin inflammatory

## Abbreviations

| | |
|---|---|
| AD | Atopic dermatitis |
| PL | Phloridzin |
| UV | Ultra violet |
| HIS | Histamine |
| HE | Hematoxylin and eosin |
| qPCR | Quantitative Polymerase Chain Reaction |
| TNF | Tumor necrosis factor |
| IL | Interleucin |
| CG | Carbomer gel |
| PL-CG | Phloridzin carbomer gel |
| DXM | Dexamethasone |
| MTT | 3-(4,5)-Dimethylthiahiazo (-z-y1)-3,5-di- phenytetrazoliumromide |
| SEM | Scanning electron microscope |
| TCS | Topical corticosteroids |
| CNIs | Calcineurin inhibitors |
| DNFB | 2,4-Dinitro-1-fluorobenzene |
| DMSO | Dimethylsulfoxide |

✉ WanYing Deng
dengwanying@gdpu.edu.cn

✉ Weiqiang Chen
cwq2187@126.com

1 School of Basic Medical Sciences, Guangdong Pharmaceutical University, Guangzhou 510006, China

2 Department of Dermatology, The First Affiliated Hospital of Guangdong Pharmaceutical University, No.19, Nonglinxia Road, Yuexiu District, Guangzhou, Guangdong, China

3 School of Nursing, Guangdong Pharmaceutical University, 280 Waihuan East Road, Guangzhou University City, GuangzhouGuangzhou, Guangdong, China

4 School of Pharmacy, Guangdong Pharmaceutical University, Guangzhou 510006, China

## Introduction

The human body is composed of many organs, with the skin occupying the largest surface area [1].The skin plays a critical role in temperature regulation, immune modulation, and barrier function, with the barrier function being particularly

Published online: 06 February 2025

crucial. When the body's immune function is compromised or the skin is subjected to disruptive factors, the likelihood of developing inflammatory skin conditions, such as atopic dermatitis and psoriasis, increases [2].Over the past few decades, the epidemiological characteristics of atopic dermatitis (AD) have undergone evolution, accompanied by emerging trends and fresh understandings of the disease burden. [3]. This trend affects not only children but also adults, with the condition persisting and becoming a chronic illness [4]. Atopic Dermatitis can cause significant personal suffering, with the primary symptoms being itchiness and dry skin [5],and it has a wide-ranging economic impact [6]. It significantly affects individuals' daily work and life. In a survey across nine European countries, the monthly cost of using moisturizers to treat atopic dermatitis exceeded the cost of medications [7].

At present, mainstream therapeutic methods include topical corticosteroids (TCS) and calcineurin inhibitors (CNIs). However, long-term or improper use of TCS and CNIs can lead to adverse events on the skin and throughout the body over time [8, 9]. Long-term use of glucocorticoids may lead to dependency. Furthermore, a questionnaire survey conducted in Sweden explored the phenomenon of topical steroid withdrawal (TSW) among patients with atopic dermatitis (AD). The findings indicated that, of the 82 participants who completed the questionnaire, 93% perceived topical glucocorticoids (TGCs) as the precipitating factor for their TSW symptoms [10].Therefore, choosing a product with high safety and no toxic side effects is particularly important.

Phloridzin, a glucoside of phloretin, has a relative molecular mass of 436.41 and a molecular formula of $C_{21}H_{24}O_{10}$, making it a dihydrochalcone substance classified under the flavonoid group. It is extracted from the connective tissue of young apple tree leaves and sweet tea. [11].Apples contain two flavonoids, phloridzin and quercetin, the latter of which has shown anti-inflammatory effects in patients with sarcoidosis and relevant animal models [12, 13].Recent studies have highlighted phloridzin's diverse pharmacological properties, particularly its significant progress in anti-inflammatory effects. For instance, it has been found to notably inhibit skin shedding damage caused by UVB irradiation in nude mice, reduce apoptosis in HaCaT cells induced by UVB, and enhance the self-repair abilities of healthy keratinocytes and fibroblasts [14]. Topical therapies are preferred in treating skin diseases, partly because they bypass first-pass elimination, allowing for direct application to affected areas, effectively targeting therapy, and significantly reduces toxic side effects [15].However, the prolonged exposure of PL to air can easily lead to the loss of moisture, thereby causing it to lose its pharmacological activity, which limits its application range.PL,combined with Carbomer 940, has been formulated into an external hydrogel dressing. This dressing not only adheres to wounds but also maintains the activity of PL, blocking direct contact between external bacteria and fungi and inflammatory wounds, which helps enhance its wound healing properties.

The main purpose of this study is to evaluate the efficacy of phloridzin, a traditional Chinese medicine monomer extracted from the natural plant apple tree, in treating atopic dermatitis.Explore the repair effect and mechanism of PL in vitro and PL-CG in vivo on the healing of chronic inflammation in mice with atopic dermatitis. To provide basic experimental evidence for the prevention and treatment of atopic dermatitis and the development of efficient and non-toxic new drugs to promote skin inflammatory healing in atopic dermatitis.

## Materials and methods

### Cell culture and treatment

HaCaT cells(cat. no. 300493; Cytion)were grown in DMEM media (Thermo Fisher Scientific, Waltham, Massachusetts, USA) supplemented with 100 U/mL streptomycin and 100 U/mL penicillin antibiotics(Thermo Fisher Scientific, Waltham, Massachusetts, USA), and 10% fetal bovine serum (FBS,Sigma-Aldrich,St. Louis, USA). The cells were cultured in a cell incubator (Thermo Fisher Scientific, Waltham, Massachusetts, USA)containing 5% carbon dioxide at 37 degrees Celsius.

PL (purity 99%, CAS: ZLSW230429-2) was purchased from Xi 'an Haoyu Kangze Biological Technology Co., Ltd. (Xi 'an, China). To control confounding factors, PL was dissolved in DMSO(dimethyl sulphoxide, inovio, USA) diluted to 0.1%.

#### Cell viability assay

HaCaT cells were cultured in T25 cell culture flasks. When the cell growth density reached 80–85%, 0.25% trypsin was added to digest the cells for 5 min, centrifuged at 1000 rpm for 2 min using a centrifuge (Thermo Fisher Scientific,Waltham, Massachusetts, USA). The HaCaT cells were then counted after resuspension in DMEM containing 10% FBS and 1% double antibiotics. After that, the cells were inoculated into 96-well plates at $1 \times 10^4$ cells per well and cultured overnight.The rest of the cells in the logarithmic growth phase were frozen and stored. The groups were set up as a Control group, a HIS group, a dexamethasone (DXM) group, and a low, medium, and high dose group of PL, respectively. In the Control group, the cells contained 0.1% DMSO and HaCaT cells, which had no killing effect on the cells, while dexamethasone (50 μmol/L) and histamine (25000 μmol/L) were added to the DXM group. The last groups were added with PL (25 μmol/L, 50 μmol/L, and

100 µmol/L) concentrations in descending order of concentration, respectively. Set up 6 replicate wells and continue to wait for 12 h of culture to observe the cell morphology of each group under an inverted microscope. 5 mg/mL MTT solution (10µL per well) was added to each well (Rsbio, Shanghai, China). The 96-well plate was shaken to make it completely homogeneous, and then put into an incubator (Thermo Fisher Scientific, Waltham, Massachusetts, USA).and continued incubation for 4 h. After adding 100 µL of DMSO to each well, the absorbance of each group was measured at 490 nm with a Microplate Reader (Biotek, Winooski, VT, USA) while gently shaking for 10 min.

Histamine configuration: 55.54 mg of histamine powder was weighed and added to 20 mL of pre-configured 10% FBS and its 1% antibiotics (100U/mL penicillin and 100U/mL streptomycin) in DMEM, at this time the concentration of 25000 µmol/L, filtrated through the 0.45um filter membrane under aseptic environment, then stored in a protected environment to keep it away from light.

The preparation method of dexamethasone is as follows: First, 100 mg of dexamethasone powder is weighed and dissolved in 2.55 mL of 0.1% dimethyl sulfoxide (DMSO) to prepare a 100 mmol/L dexamethasone solution. Subsequently, 1 µL of this solution is withdrawn and added to 999 µL of Dulbecco's Modified Eagle Medium (DMEM) to achieve a 1000-fold dilution, thereby obtaining a 100 µmol/L dexamethasone solution. Further, by half-diluting this solution, the concentration of dexamethasone is adjusted to 50 µmol/L. Lastly, the solution is filtered through a 0.45-µm filter in a sterile environment and stored in darkness for future use.

The PL solution is prepared as follows Measure 111.28 mg of PL extract powder and dissolve it in 2.55 mL of 0.1% DMSO. From this solution, 1 µL is taken and mixed with 999 µL of DMEM to obtain a 1000-fold dilution, giving a concentration of 100 µmol/L. The concentration of PL solution is then adjusted to 25 µmol/L,50 µmol/L and 100 µmol/L by stepwise dilution. Finally, the PL solution is filtered through a 0.45-micron filter in a sterile environment and then stored in the dark for subsequent experiments.

### RNA extraction from cells and quantitative polymerase chain reaction (q-PCR).

Evaluation of IL-1β, IL-6, IL-8, and mRNA expression in cells was conducted by isolating total RNA using the RNAsimple Total RNA Kit (Tiengen Biotechnology, Beijing, China) following the manufacturer's instructions. Reverse transcription was performed with the iScript cDNA Synthesis Kit (BioRad, Hercules, California, USA). The resulting cDNA was amplified using a real-time PCR system (qTOWER, Analytik Jena GmbH, Jena, Germany). The thermal cycling conditions were as follows: initial denaturation and enzyme activation at 95 °C for 2 min (1 cycle), followed by 40 cycles of 95 °C denaturation for 10 s, 60 °C annealing for 15 s, and 72 °C extension for 30 s. The iQ SYBR Green Supermix (BioRad, Hercules, California, USA) was used. At the end of the cycles, a melting curve analysis was performed to ensure the absence of non-specific products. The relative mRNA expression levels were normalized to GAPDH as the internal control to standardize differences. The primer sequences are shown in Table 1.

### Preparation of sensitizing solution and PL-CG

Acetone and olive oil were prepared in the ratio of 3:1. Then 2,4-dinitro-1-fluorobenzene (DNFB) was added into the sensitization solution to form a concentration of 0.3% and 0.1%, respectively. The 0.3% DNFB solution was configured as a high-concentration sensitizer for the first excitation of mouse skin, and 0.1% DNFB was used for the subsequent low-concentration maintenance. Carbomer 940 (Meilunbio, Dalian, China) is mild in nature, does not irritate the skin, and was used as a carrier for herbal medicine in this study. Firstly, 3 g of carbomer was weighed and mixed with ultrapure water while stirring. The PH was then adjusted to 7.0 using triethanolamine solution. Subsequently, three different concentrations of phlorizin were added to the carbomer gel, with constant stirring throughout the addition process. Final concentrations of 0.5%, 1%, and 2% PL-CQ were prepared.

### Establish DNFB-induced atopic dermatitis mouse model and related treatment

All animal procedures were conducted in compliance with the Guidelines for the Care and Use of Laboratory Animals issued by Guangdong Pharmaceutical University. These procedures were approved by the Animal Ethics Committee (Approval Number: gdpulacspf2022277) and strictly adhered to the guidelines set forth by the International Council for Laboratory Animal Science (ICLAS). All animal experiments were designed to minimize animal suffering and ensure appropriate humane endpoints were implemented at

**Table 1** Primers used forRT- qPCR

| | |
|---|---|
| hIL8-F | GGTGCAGTTTTGCCAAGGAG |
| hIL8-R | TTCCTTGGGGTCCAGACAGA |
| hIL6-F | CACAGACAGCCACTCACCTC |
| hIL6-R | GCCTCTTTGCTGCTTTCACA |
| hIL1β-F | GACACATGGGATAACGAGGCT |
| hIL1β-R | TGGACCAGACATCACCAAGC |
| GAPDH-F | AGACCTGTACGCCAACACAG |
| GAPDH-R | CCAGGGCAGTGATCTCCTTC |

the conclusion of the experiments.Animals were raised in SPF environment(body weight, 18 ± 2 g),with room temperature 26℃ and relative humidity 70%, in the Animal Experimental Center of Guangdong Pharmaceutical University, a 12 h day/night alternation system was implemented.The animals were allowed to feed ad libitum. Drinking water, feed and bedding were changed regularly as scheduled. After being transferred to the animal house, the mice were first subjected to a one-week environmental acclimatization period and their backs were dehairing the night before molding. According to the experimental design, a total of 42 BALB/c mice aged 6 to 8 weeks were divided into 7 groups with 6 mice per group by random number table method. The grouping is as follows: control group, DNFB group, CG group, positive drug group, and groups with different concentrations of 0.5% PL-CG, 1% PL-CG, and 2% PL-CG. In all groups except the control group, DNFB was applied to the ears and backs of the mice. In the experimental design of this study, the modeling process was initiated on the first day by externally applying 0.3% dinitrofluorobenzene (DNFB) solution on the dorsum (10μL) and left ear (3μL) of the mice. Subsequently, on the fifth day, the dorsum (10μL) and left ear (3μL) were re-sensitised with 0.1% DNFB solution. This model-building procedure was performed every two days from the first day and continued until the fourteenth day. From the fifth day onwards, a daily treatment regimen was adopted.After the DNFB application was completed, all mice, except for the blank control and model groups, received the corresponding doses of therapeutic drugs externally on their ears and backs according to their assigned groups.PL and DXM groups were treated with carbomer gel and dexamethasone ointment, respectively. Meanwhile, in order to record the skin response, the skin condition of mice was recorded using photography in the same direction. Caseviewer (Version 2.4; 3DHISTECH, Budapest, Hungary) was used and the healing rate of back wound was calculated. In addition, After the treatment, the mice were placed in equal-sized clear plastic boxes, videotaped for 10 min and recorded how often the mice scratched their backs.At the predetermined endpoint, the concentration of isoflurane is cautiously adjusted to 5%. The purpose of this step is to ensure that the mice can swiftly and painlessly enter a deep state of anesthesia, preparing them for the subsequent euthanasia process. It is noteworthy that the concentration should be adjusted slowly, with continuous monitoring of the mice's reactions. Following the significant slowing and eventual cessation of the mice's breathing, they must remain exposed to the 5% isoflurane concentration for an additional period of not less than one minute. This extended exposure time is to ensure that the mice have definitively lost all vital signs, thereby confirming their death. During this process, close attention should be paid to any minute reactions of the mice to guarantee the completeness of euthanasia.Once the mice are confirmed dead, the anesthetic gas supply system is immediately shut off to prevent unnecessary leakage of anesthetic gas. Simultaneously, ventilation equipment is activated to rapidly clear the anesthetic gas from the experimental area, ensuring the safety of the experimental personnel. Subsequently, the euthanized mice are properly disposed of, including transferring them to a designated disposal area and following the laboratory's protocols for storage or further processing. Additionally, the anesthesia equipment and containers used are thoroughly cleaned and disinfected to prevent cross-contamination and pollution.Before preparing for dissection, the skin tissue of the mice is removed in a sterile environment. This step strictly adheres to sterile operating procedures to ensure the cleanliness and accuracy of the dissection process. In a sterile environment, it is necessary to wear sterile gloves, masks, and hats, and to use sterile instruments and disinfectants. During the dissection, constant vigilance is maintained to avoid any potential contamination of the surrounding environment. This includes preventing the spilling of dissection fluids or the dropping of tissue fragments, and promptly cleaning up and neutralizing any potential contaminants. At the same time, the accuracy and reliability of the dissection results are ensured by carefully observing and recording every detail of the dissection process.Finally, after extracting the required tissues in a sterile environment, the carcasses of the mice undergo high-temperature and high-pressure sterilization. This step aims to completely eliminate any microorganisms or pathogens that may be present on the carcasses, thereby preventing potential hazards to the environment and personnel. All of the above steps conducted in strict adherence to the ICLAS guidelines and relevant ethical requirements, ensuring that animals experience minimal pain during the experiment and their lives are respected.

### RNA extraction from animal tissues and RT-qPCR

In a comprehensive evaluation of skin tissue, we assessed the levels of the key inflammatory cytokines IL-1β, IL-6, TNF-α, and their corresponding mRNA expression. RNA is carefully isolated from skin tissue samples using the rnasimple Total RNA Kit, which is based on the detailed operation manuals provided by the manufacturer, which extensively explain each step's operation methods. We utilized the iScript cDNA synthesis kit for reverse transcription, strictly adhering to the kit's instructions. Subsequent amplification was carried out using a Quantitative real-time PCR system. The thermal cycling conditions are strictly followed to ensure accuracy. The specific steps are as follows: initial denaturation and enzyme activation at 95℃ for 2 min, denaturation at 95℃ for 10 s, annealing at 60℃ for 15 s, extension at 72℃ for 30 s, and a total of 40 cycles are repeated. The use of BioRad's iQ SYBR Green Supermix is an integral

part of this process. At the critical moment when the cyclic reaction finally ends, it is essential to obtain melting curves with high accuracy and fine detail. This step is crucial as it ensures that no nonspecific products are present during the experiment, thereby guaranteeing the reliability and accuracy of the experimental results. By carefully analyzing the melting curves, it is possible to effectively monitor and evaluate the specificity of the reaction at each stage of the experiment, ensuring that the final data obtained possesses high reliabilities and validities. This step is crucial for ensuring the precision and reliability of scientific research. The relative expression of mRNA is standardized to GAPDH as the endogenous control. During the experimental process, we used a specific set of primer sequences, which are listed in Table 2 for reference.

### Histopathological examination

Skin tissues were sampled, fixed in 4% paraformaldehyde, sectioned, stained in 0.5% eosin solution and fixed in neutral gum. Finally, photographs were taken under a light microscope and epidermal thickness was measured using Caseviewer (Version 2.4; 3DHISTECH, Budapest, Hungary).

**Table 2** The situation regarding PCR primers

| | |
|---|---|
| mIL8-F | CATCTTCGTCCGTCCCTGTG |
| mIL8-R | TCACTTCCTTTCTGTTGCAGT |
| mIL1β-F | AACCTTTGACCTGGGCTGTC |
| mIL1β-R | AAGGTCCACGGGAAAGACAC |
| mTnf-α-F | CACCGTCAGCCGATTTGCTA |
| mTnf-α-R | TTGGGCAGATTGACCTCAGC |
| mIL6-F | ATCCAGTTGCCTTCTTGGGA |
| mIL6-R | GGTCTGTTGGGAGTGGTATCC |
| GAPDH -F | CTGAGAGGGAAATCGTGCGT |
| GAPDH -R | AGGAAGGCTGGAAAAGAGCC |

### Scanning electron microscope analysis(SEM)

First, PL solutions of different concentrations were added to 940 carbomer, and then left for one night to expand overnight. The next day, put the ice in the freezer compartment of the refrigerator. (SIEMENS AG, Munich, Germany) to below freezing point and use a vacuum lyophilizer (SP Scientific, New York, USA) to convert the ice into water vapor at a higher vacuum and remove the waste gas. The last solid is frozen and dried again. After soaking the material in liquid nitrogen (Dejie Force Metal Technology Co., LTD, Shenzhen, China) for 3 min, the material is broken off to obtain the section, part of the solid is intercepted, and gold foil is sprayed on the cross section to increase the conductivity, and then SEM (tescan vega3,Shanghai, China) pictures are taken.

### Viscosity measurement

The viscosity of all the gels was determined at 25 ± 2 ℃ using Brookfield viscometer fitted with spindle S64, 5 rpm. (Model: DV-II Pro; Brookfield Engineering Laboratories, MA, USA). Viscosity of each gel was determined three times.

### stability test

In order to further prove the stability of 2% PL-CG, it is necessary to determine whether PL-CG can maintain a gel-like form without liquefying or drying out under normal temperature conditions. Under this requirement, the following experiments need to be carried out (Table 3).

2.2.1The Influence of Carbomer Gels with Different Concentrations on Drug Release.

In order to maintain the sink condition, PBS buffer (0.02 mol·$L^{-1}$) with a pH of 7.0 containing 30% (v/v) ethanol was used as the release medium. The in vitro release behaviors of 2% PL and PL-CG with different amounts of CG added were investigated by the dialysis method.Appropriate amounts of PL-CG were weighed respectively and then added into pre-treated dialysis bags (molecular cut-off:

**Table 3** Stability Test for 2%PL-CG

| Stability Test Name | Procedure |
|---|---|
| High-speed Centrifugation Test | Put an appropriate amount of the drug gel sample into a centrifuge tube, and then conduct centrifugation at a rotational speed of 3,500 revolutions per minute for 15 min. During this process, pay close attention to the stratification phenomenon of the gel and the subtle changes in its appearance |
| Alternating Heat and Cold Test | Take an appropriate amount of the drug gel sample and put it into a centrifuge tube, and then place it in a refrigerator at −20 °C for refrigeration for 20 h. After refrigeration, put it into an electric constant-temperature water bath at 60 °C and keep it at a constant temperature for 2 h, and evaluate whether its appearance has changed |
| Different pH Value Experiment | Set the pH values to 4.0, 7.0, and 10.0 respectively, and evaluate whether its appearance has changed |

10 kDa). After sealing both ends of the dialysis bags, they were placed into the release medium (900 mL). The temperature was maintained at 37 °C and the rotation speed was set at 100 r·min$^{-1}$. Samples of 2 mL were taken at time points of 1, 2, 4, 6, 8, 10, and 12 h respectively. Meanwhile, 2 mL of fresh release medium was replenished at the same time. After the samples were centrifuged at 10,000 r·min$^{-1}$ for 10 min, the supernatants were taken to detect the absorbance at 280 nm so as to determine the content of PL, calculate the cumulative release rate, and draw the release curve. Each group of experiments was carried out in parallel for three times.Furthermore, the release situations of PL-CG with different concentrations of CG in the above-mentioned release medium were fitted with mathematical models to investigate the release pattern of phlorizin. Commonly used release kinetic mathematical models include the zero-order release model, the first-order release model, the Higuchi model, and the Weibull model.

#### Statistic analysis

The results were reported as mean values ± standard deviations (SD).Statistical significance was assessed using either one-way ANOVA followed by Tukey's post-hoc test or an unpaired t-test assuming that both populations have the same standard deviation. Performed with GraphPad Prism 8.0 software, considering $P < 0.05$ as the threshold for significance. Each experiment was conducted three times, encompassing both biological and technical replicates.

## Results

### Effect of PL on HaCaT cell viability

To determine the safe and non-toxic range of phloridzin in HaCaT cells, an MTT assay was conducted to assess the impact of PL on HaCaT cell viability. The results showed no significant impact on cell viability(ns).Therefore, the safe and non-toxic range of PL was determined to be 6.25 µmol/L to 100 µmol/L (Fig. 1).

### Effect of histamine on the survival rate of HaCaT cells

To identify the optimal inflammatory model with a cell survival rate of approximately 50%, varying concentrations of histamine (HIS) were administered to HaCaT cells and cultured for 12 h and 24 h (Fig. 2A, B), respectively. The results showed that the average cell survival rate was 50.22% after 12 h of exposure to 25000 µmol/L of HIS(Fig. 2A),consequently, a concentration of 25000 µmol/L HIS was added to HaCaT cells and cultured for 12 h ($P < 0.001$), which proved to be the ideal dose and duration for the cell inflammation model.

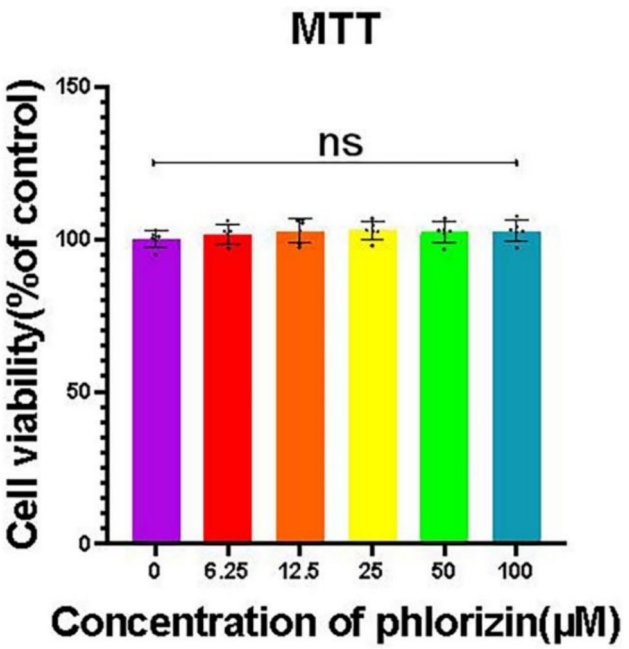


**Fig. 1** Effect of PL on survival rate of HaCaT cells. (***$P < 0.001$,**$P < 0.01$, *$P < 0.05$,ns > 0.05)

#### Effect of PL on the proliferative activity of inflammatory cells

To assess the potential protective effect of PL on histamine-induced HaCaT cells, an MTT assay was conducted to measure its impact on cell survival under HIS induction (Fig. 3). The results showed a marked decrease in the survival rate of HaCaT cells after HIS induction compared to the Control group ($P < 0.001$). Specifically, there was a significant difference in cell survival rates between the 50 µmol/L and 100 µmol/L PL groups compared to the Model group ($P < 0.001$). Additionally, the 50 µmol/L DXM group showed a significant improvement following treatment ($P < 0.05$). Furthermore, a statistically significant difference ($P < 0.05$) was observed between the 100 µmol/L PL group and the DXM group, indicating that PL exerted a superior protective effect on histamine-induced HaCaT cells compared to DXM.These findings suggest that PL exhibits protective effects on histamine-induced HaCaT cells, and the therapeutic efficacy of the 100 µmol/L PL group was superior to that of the DXM group ($P < 0.05$). This demonstrates the potential of PL as a protective agent against histamine-induced cell damage.

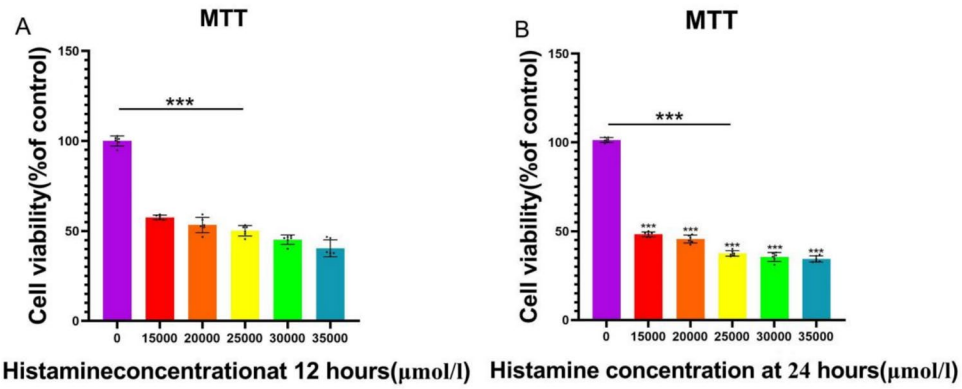


**Fig. 2** The viability of HaCaT cells cultured with histamine at various concentrations for 12 h. **A** The viability of HaCaT cells cultured with histamine at various concentrations for 24 h. **B** (***$P < 0.001$,**$P < 0.01$, *$P < 0.05$,ns > 0.05)

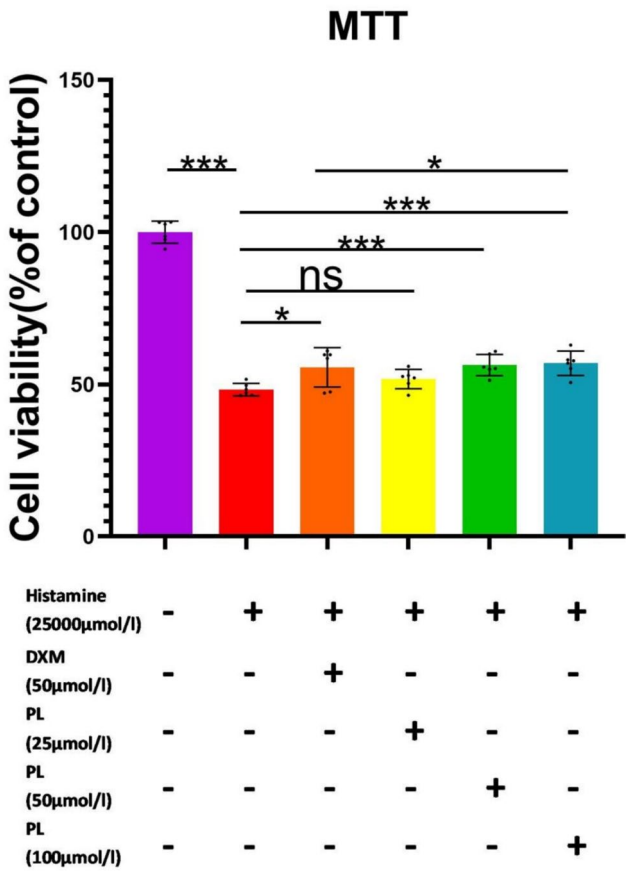


**Fig. 3** Effect of PL on HaCaT cells.(***$P < 0.001$,**$P < 0.01$,*$P < 0.005$, ns > 0.05, + :Positive, - :negative)

## Expression levels of IL-1β, IL-6 and IL-8 mRNA in cells

To examine whether Phloridzin can inhibit the increase of inflammatory factor mRNA in HaCaT cells, we employed qPCR to assess the effect of phloridzin on the expression of inflammatory factor mRNA induced by histamine (Fig. 4A–C). Compared to the Control group, treatment with 25000 μmol/L HIS significantly elevated the mRNA levels of IL-1β, IL-6, and IL-8 in cells($P < 0.001$). However, treatment with 50 μmol/L phloridzin, 100 μmol/L phloridzin and Dexamethasone significantly reduced the mRNA levels of these inflammatory cytokines($P < 0.001$), thereby mitigating the inflammatory response.

### Effect of phloridzin on the degree of ear swelling in AD mice

After the treatment period, ear thickness was measured using vernier calipers. The left ear of the mice in the DNFB group was visibly thickened, with a significant difference in thickness compared to the right ear (Fig. 5A). On day 14, the left ear thickness in the DNFB group was notably greater than that in the Control group.Dexamethasone and carbomer gel were applied to the left ear of mice in the DNFB and CG groups, respectively, following modeling. The DXM group showed significant improvement compared to the DNFB group ($P < 0.05$). Treatment with 2% PL was also highly effective compared to the DNFB group ($P < 0.001$), exhibiting a dose-dependent effect. These results indicate that PL alleviated epidermal inflammatory swelling and enhanced skin tissue recovery in the treatment of atopic dermatitis (Fig. 5B).

## Effect of PL on skin inflammatory healing and pruritus of back skin in mice

After treatment, the back skin of mice in the Control group showed no significant changes. In contrast, mice in the DNFB group, following solvent stimulation, displayed clear erythema, lichenification, scabbing, and epidermal shedding on their back skin. The inflammatory area was markedly increased($P < 0.001$).The DXM group exhibited some improvement in skin lesions compared to the DNFB group. Additionally, significant improvements were observed in the skin lesions of the 0.5% PL-CG, 1% PL-CG, and 2% PL-CG groups, with a notable reduction in the area of inflammation

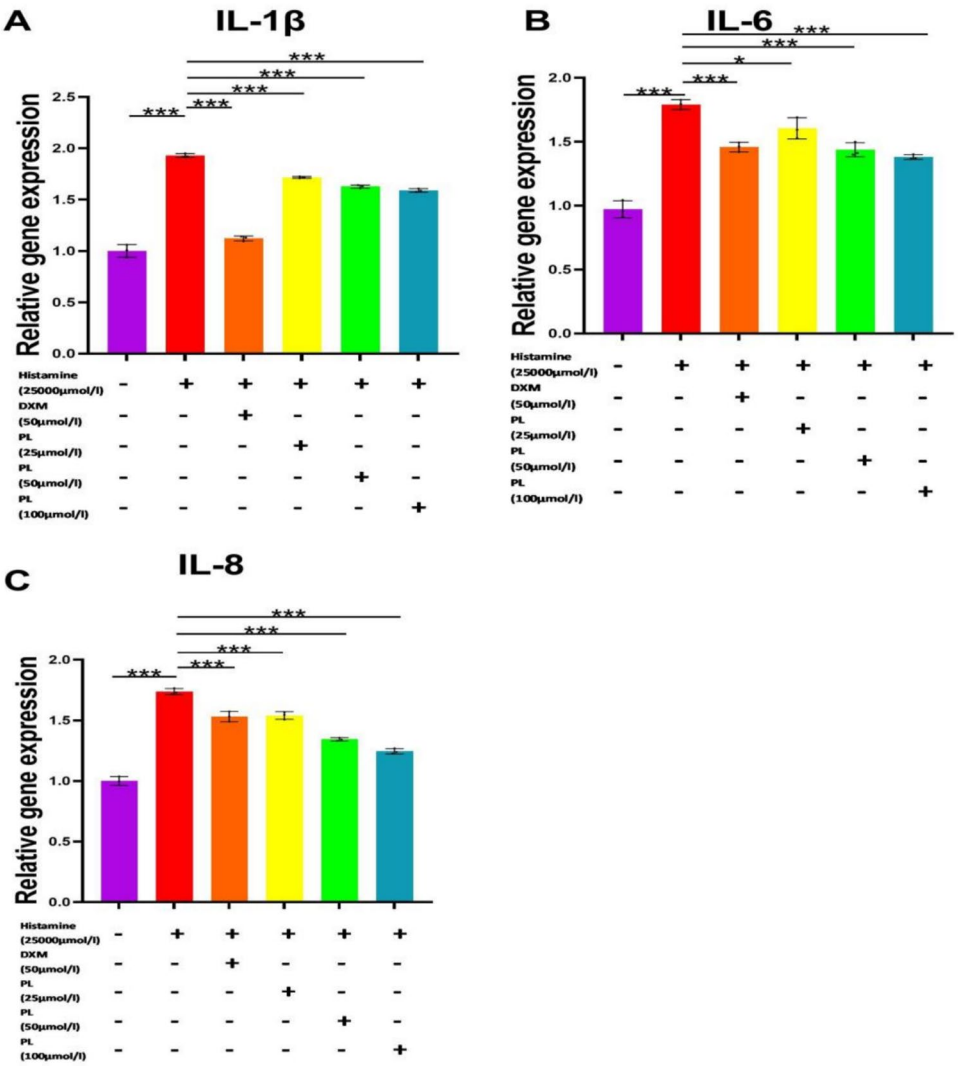


**Fig. 4** The mRNA levels of IL-1β, IL-6, and IL-8 in cells. (4A–C). PL inhibits mRNA expression of histamine stimulating HaCaT secretion of inflammatory factors. (***$P<0.001$,**$P<0.01$,*$P<0.05$, +: Positive, −: negative)

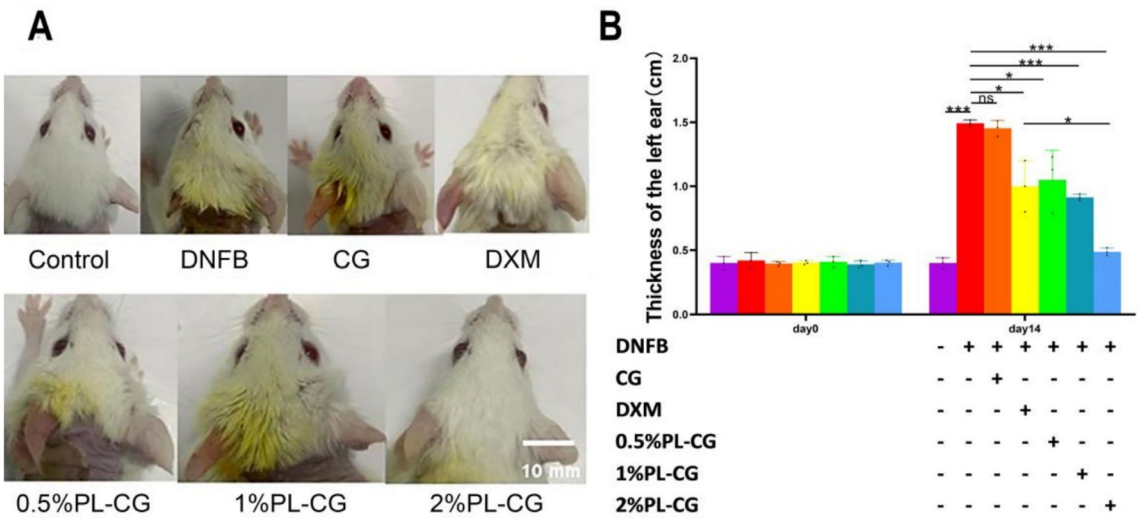


**Fig. 5** Skin damage condition in the ear and auricular thickness of the left ear in each group of mice. (5A、B) (***$P<0.001$,**$P<0.01$,*$P<0.05$, ns > 0.05, +:Positive,-:negative)

(P < 0.001). These findings demonstrate that PL-CG effectively improved skin lesions in AD mice (Fig. 6A, B).

Atopic Dermatitis is often associated with skin itching, and to evaluate the severity of the condition in mice, the number of back scratches was visually counted. On days 7 and 14, the DNFB group exhibited a significantly higher number of scratches within a 10 min period compared to the Control group (P < 0.001), indicating increased levels of itching in the DNFB group. In contrast, mice treated with 2% PL-CG showed a significant reduction in scratching frequency within the same timeframe compared to the DNFB group (P < 0.001), with symptoms of scratching gradually alleviating over time. These results demonstrate that PL-CG effectively relieves pruritus in mice with atopic dermatitis (Fig. 7).

## Inflammatory skin tissue hematoxylin eosin staining results

To investigate the skin inflammatory healing effect of PL-CG, HE staining was used to evaluate the recovery of skin tissue on the backs of mice at the end of the treatment. The epidermal cell structure on the backs of mice in the Control group appeared normal, with no inflammatory reactions observed across all layers of the epidermis, and no signs of edema, congestion, or inflammatory cell infiltration. After the model induction, the pathological changes of the back lesions in the DNFB group showed obvious chronic inflammatory hyperplasia, increased epidermal and dermal thickness, accompanied by hyperkeratosis and hypokeratosis. The epidermal thickness was significantly higher than that in the Control group, with spinous layer hyperplasia

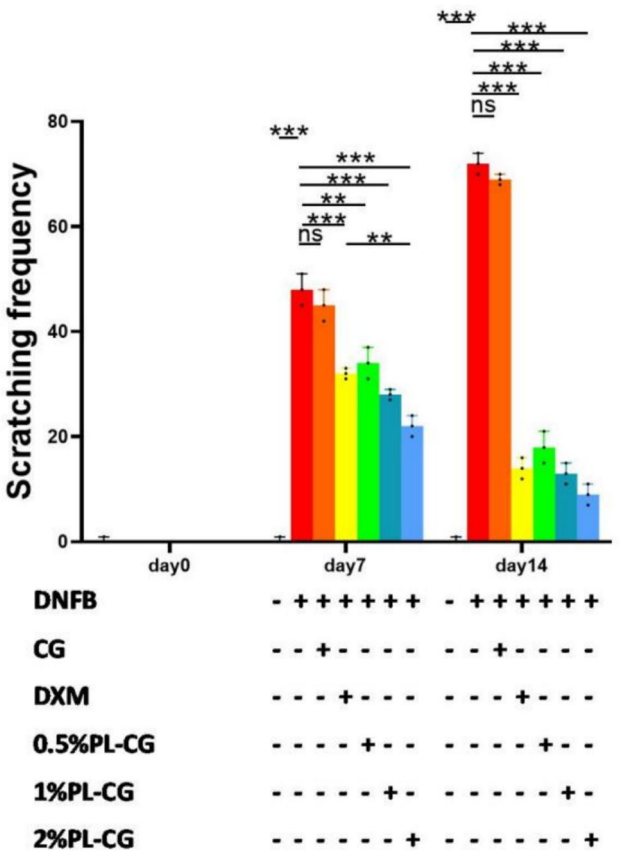


**Fig. 7** Frequency of back scratching in mice.(***$P < 0.001$,**$P < 0.01$,*$P < 0.05$, ns > 0.05, + :Positive, −:negative)

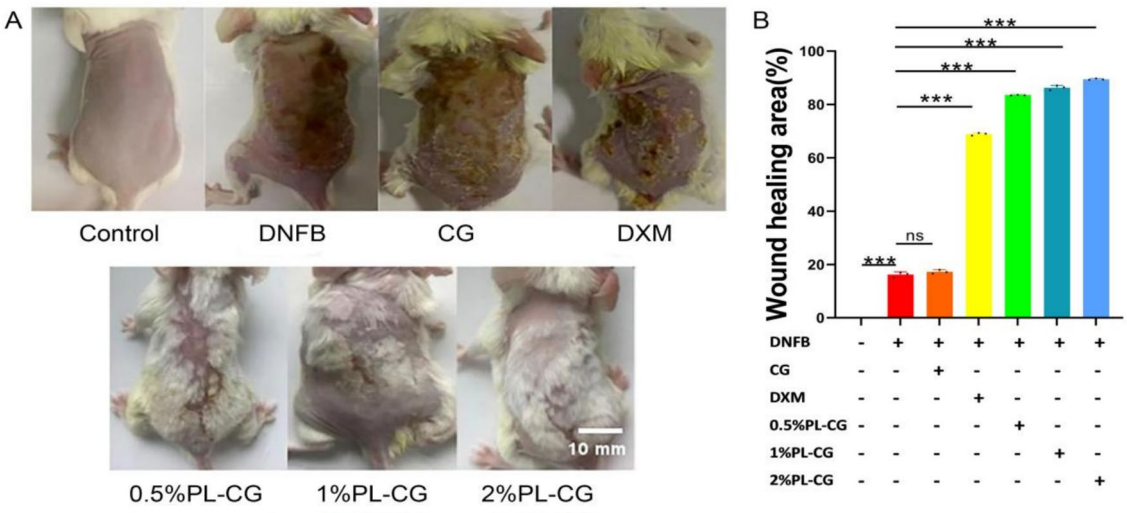


**Fig. 6** The skin condition of the back of mice in each group was observed at the end of treatment. (6A)(scale bar, 10 mm).The skin wound healing rate of mice in each group was calculated at the end of treatment.(6B) (***$P < 0.001$,**$P < 0.01$,*$P < 0.05$, ns > 0.05, + :Positive,-:negative)

(P < 0.001).Compared to the DNFB group, the epidermal thickening decreased in the DXM (P < 0.001), 0.5% PL-CG, and 1% PL-CG groups (P < 0.01), with the most significant reduction observed in the 2% PL-CG group (P < 0.001). These results demonstrate that PL-CG significantly reduces inflammatory cell infiltration and markedly decreases epidermal thickness (Fig. 8A, B) (scale bar, 100 μm).

## Expression levels of IL-1β, TNF-α, IL-6 and IL-8 mRNA in skin tissue.

To assess the ability of PL-CG to prevent the increase of inflammatory factors in atopic dermatitis mice, RT-qPCR was used to measure its impact on the mRNA levels of IL-1β, IL-6, IL-8, and TNF-α in DNFB-induced atopic dermatitis mice.DNFB induction significantly elevated the mRNA expression levels of these inflammatory cytokines (IL-1β, IL-6, IL-8, and TNF-α) (P < 0.001). In the 1%PL-CG 、2%PL-CG and DXM groups, the mRNA levels of IL-1β, IL-6, IL-8, and TNF-α were reduced, effectively alleviating the inflammatory response (P < 0.001).Moreover, the PL-CG group exhibited a dose-dependent effect, with increasing concentrations of PL-CG leading to greater reductions in the mRNA levels of the inflammatory cytokines (Fig. 9A–D). These results indicate that PL-CG effectively attenuates the upregulation of pro-inflammatory mediators in the DNFB-induced atopic dermatitis mouse model.

### PL-CG scanning electron microscope observation

Samples of 0.5%, 1%, and 2% PL-CG were analyzed using a scanning electron microscope. The results revealed that the microstructure of PL-CG at different concentrations was consistent, exhibiting a loose and porous network. This structure is beneficial for enhancing skin surface adsorption and promoting cell infiltration(Fig. 10A-C).

## Results of viscosity measurement

The study found that carbomer 940 with a concentration of 1% can be used to prepare a drug-loaded gel with ideal rheological properties. It enables the gel to have good adhesiveness, allowing it to adhere to the skin surface and prolong the drug's action time (Table 4).

## Stability test for PL-CG

After the High-speed Centrifugation Test and the Alternating Heat and Cold Test, 2% PL-CG showed a good homogenization effect, without stratification, color change or abnormal changes in appearance. As shown in Fig. 11, after undergoing the above high-speed centrifugation experiment (Fig. 11A) and alternating heat and cold experiment (Fig. 11B), 2% PL-CG presented a uniform texture and was not prone to deterioration.It can be seen from Table 5 that 2% PL-CG did not experience stratification or color changes

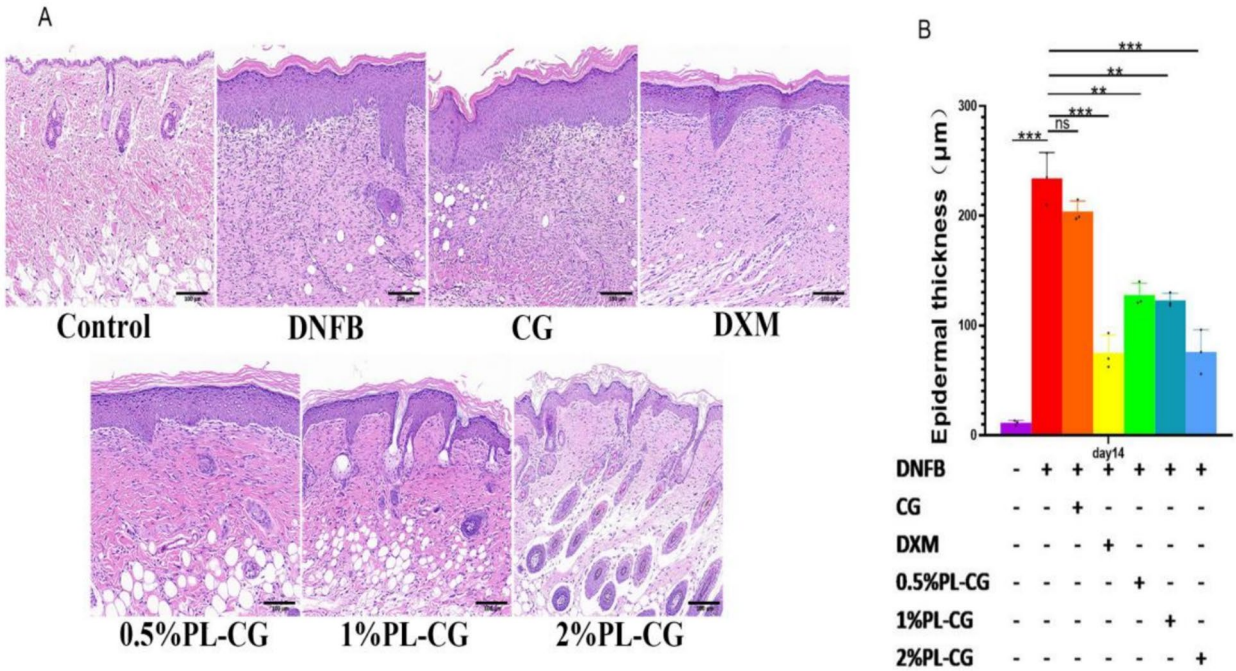


**Fig. 8** HE staining and epidermal thickness measurement of back skin of Atopic Dermatitis mice. (8A, B). (***$P < 0.001$,**$P < 0.01$,*$P < 0.05$, ns > 0.05, + :Positive, −:negative,magnifications, 10X)

and the like in the above experiments.After PL-CG was subjected to tests under different pH values, it was found that when the pH value was 4.0, the gel had a thin texture and strong fluidity and could not stay on the skin surface for a long time. When the pH value was 10.0, the gel had poor fluidity and part of its transparency decreased, which affected the observation of skin outcome indicators. When the pH value was 7.0, the fluidity of carbomer was neither too thin due to excessive acidity, resulting in rapid drug release and failure to achieve the sustained-release effect, nor too viscous due to excessive alkalinity, which would affect the spreading on the skin at the administration site and the drug release (Fig. 12).

### Results of the influence of carbomer gels with different concentrations on drug release

Compared with the PL ethanol solution, the cumulative release rate of PL-CG in the release medium within 12 h was significantly reduced, which indicates that carbomer has a sustained-release effect.Furthermore, compared with PL, PL-CG with different CG contents exhibited further sustained-release characteristics in the medium solution. And its cumulative release rate decreased as the CG content increased when the CG content exceeded 1%. This suggests that PL-CG with an excessive CG content can form a denser three-dimensional network structure, which has a stronger blocking effect on the release of PL (Fig. 13). It can be known from Table 6 that by comparing the correlation coefficient $R^2$ values of the fitting equations of different mathematical models, it was confirmed that the release models of all systems in the release medium conformed to the first-order release, Higuchim, and Weibull equations.The $R^2$ of the first-order release equation fluctuated to a certain extent with the increase in the CG addition amount. When the CG addition amount was 0, it was 0.97728, indicating that when there was no CG or the addition amount was very small, the drug release might conform to the first-order release kinetics to some extent.The $R^2$ of the Higuchi equation reached the highest value of 0.98223 when the CG addition amount was 0.25. When the CG addition amount was relatively low, the $R^2$ increased with the increase in the addition amount. This might be because the addition of CG improved the drug diffusion environment, making the drug release more in line with the diffusion-based Higuchi equation. However, when the addition amount continued to increase, the $R^2$ did not continue to rise. This might be because other release mechanisms (such as the swelling of CG, etc.) began to have an impact on the drug release, resulting in the inability of the diffusion-based Higuchi equation to fit well.The $R^2$ of the Weibull equation was quite high under various CG addition amounts, and the fluctuation was relatively small with the change in the addition amount. This further proves the stability and accuracy of the Weibull equation in describing the release behavior of CG. No matter how the CG addition amount changes, the Weibull equation can better adapt to and fit the drug release data.

## Discussion

Phloridzin is a polyphenolic compound derived from natural plants, exhibiting a range of biological activities including antioxidant [16], anti-inflammatory [17], antidiabetic [18], anti-depression [19]and anti-aging effects [20] [21]. It is widely applied in various research fields related to different diseases. However, the mechanisms of action and safety of Phloridzin in treating atopic dermatitis remain unclear. Our study found that phloridzin is safe and non-toxic to HaCaT cells at concentrations ranging from 6.25 μmol/L to 100 μmol/L (Fig. 1).

Histamine is a neurotransmitter commonly found in human tissues that promotes inflammation and is formed through the decarboxylation of histidine. It participates in immune regulation and inflammatory responses through four different receptor types: H1, H2, H3, and H4. Specifically, studies have shown that the H4 receptor plays a crucial role in mediating the inflammatory effects of chronic inflammatory skin diseases [22–24].Research indicates that histamine can enhance the secretion of Th2 cytokines, including interleukin IL-4 [25]. In mice, histamine can induce the generation of interleukin IL-6 and the synthesis of tumor necrosis factor TNF-α [26, 27]. TNF-α inhibits the differentiation of myofibroblasts, thereby prolonging the duration of inflammation, which may ultimately lead to a decrease in wound healing speed [28]. Therefore, effective inhibition of inflammatory factors becomes essential. The results of this study demonstrate that when Histamine is treated on HaCaT cells for 12 h at a concentration of 25000 μmol/L, it exhibits a cytotoxic effect on HaCaT cells (Fig. 2A). Phloridzin shows a protective effect on histamine-induced HaCaT cells (Fig. 3) and effectively inhibits the mRNA expression of inflammatory factors (Fig. 4A–C).

To investigate the effects of PL-CG on the pathogenesis of atopic dermatitis in mice, this study further conducted in vivo experiments and successfully established an atopic dermatitis mouse model. After being treated with DNFB sensitization liquid, the mice's skin gradually presented with dry peeling, yellow inflammatory exudate, and scab formation. Moreover, the hair in the scab area appeared sparse and dull in color. The experimental results indicated that the ear cartilage thickness of mice in the 0.5% PL-CG, 1% PL-CG, and 2% PL-CG treatment groups decreased significantly compared to the DNFB treatment group (Fig. 5A). The wound area also displayed a smaller size (Fig. 6A). Based on the data analysis of the ear cartilage thickness (Fig. 5B) and

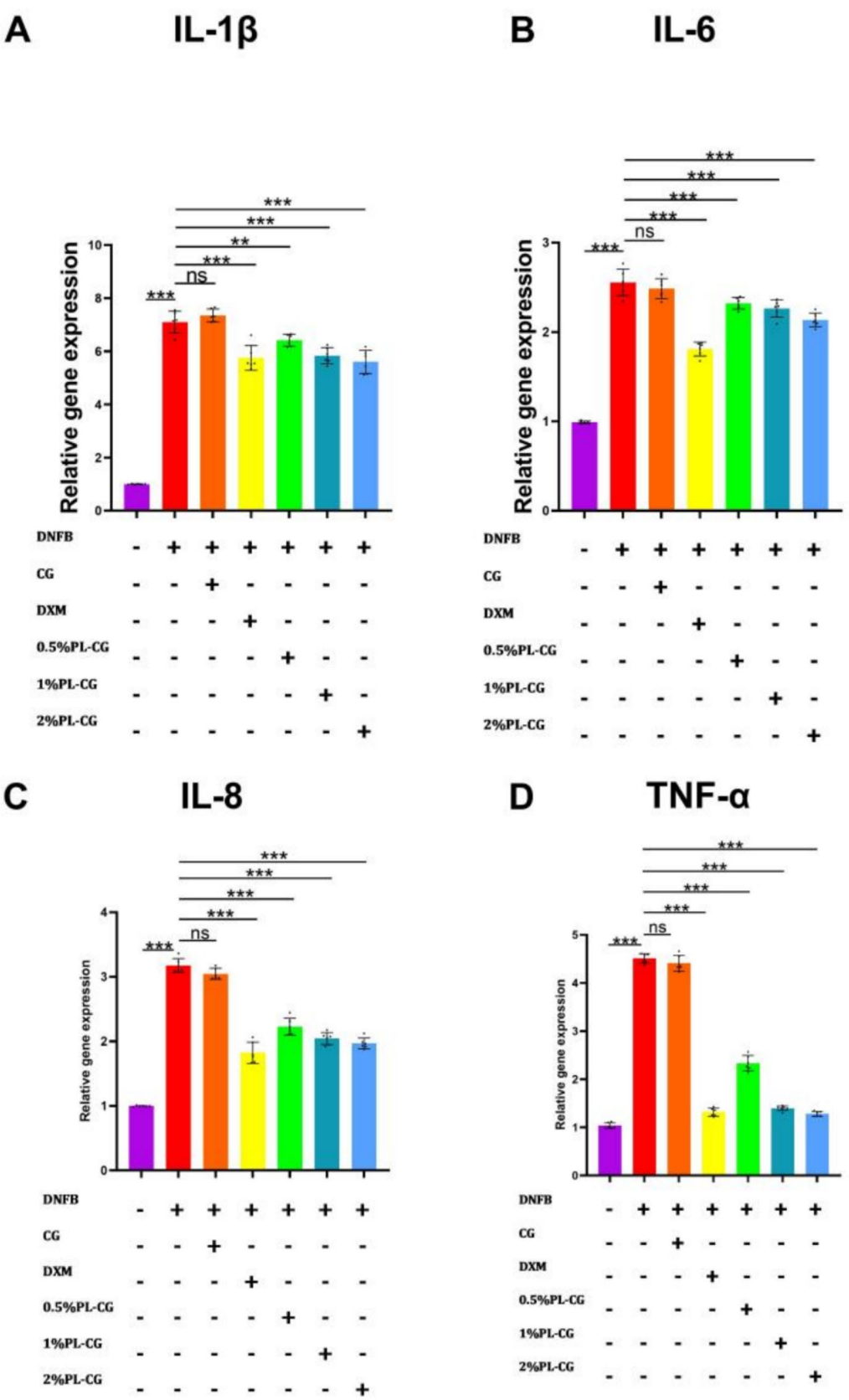
A
IL-1β
B
IL-6
C
IL-8
D
TNF-α
Relative gene expression
ns
***
**
DNFB
CG
DXM
0.5%PL-CG
1%PL-CG
2%PL-CG

◂**Fig. 9** The impact of PL-CG on the expression level of mRNA in the skin injury tissue of Atopic Dermatitis mice. (8A-D).IL-1β mRNA expression levels in each group of mice (**A**); IL-6 mRNA expression levels in each group of mice (**B**); IL-8 mRNA expression levels in each group of mice (**C**) TNF-α mRNA expression levels in each group of mice (**D**) (***$P < 0.001$,**$P < 0.01$,*$P < 0.05$, ns > 0.05, + :Positive, −:negative)

the skin inflammatory healing progress (Fig. 5C), we can deduce that the 1% PL-CG group and the 2% PL-CG group exhibited better healing effects than the DXM treatment group. It is reassuring that the 2% PL-CG group exhibited the most effective skin inflammatory healing, with nearly complete epidermal formation.

To investigate the role of PL-CG in skin inflammatory healing, we collected mouse skin tissues for histological analysis. Following wound formation, the organism enters the inflammatory response phase, releasing inflammatory mediators to stimulate local inflammatory reactions [29]. Subsequently, the skin inflammatory healing process begins, closely associated with the formation of granulation tissue, re-epithelialization, and wound contraction [30].In the initial stages of skin inflammatory healing, granulation tissue production predominates, occurring concurrently with re-epithelialization. During this process, keratinocytes in the basal layer of the epidermis contribute to re-epithelialization by proliferating and migrating to restore the epidermal barrier function. This is followed by wound contraction, resulting in the formation of a new epidermal layer. In the later stages of skin inflammatory healing, known as the remodeling phase, newly formed blood vessels gradually regress and disappear, leading to a significant reduction in the area of injury, thereby achieving effective skin inflammatory healing. Histopathological examination (HE staining) revealed that the dorsal skin of mice in the model group exhibited hyperkeratosis or disruption of the skin barrier following DNFB exposure ($P < 0.001$).Compared to the DNFB group, the CG group did not show significant improvement or signs of wound remodeling. In contrast, mice treated with DXM and PL-CG (0.5%, 1%, and 2%) exhibited notable improvements in their dorsal skin lesions. Notably, in the mice treated with 2% PL-CG, the epidermal and spinous layer thicknesses at the injured site were significantly reduced. The infiltration of inflammatory cells in the dermis was also significantly decreased, leading to the formation of an epidermis resembling normal morphology, a marked improvement (Fig. 8A, B). These results indicate that PL-CG can significantly improve skin lesions in AD mice and promote the re-epithelialization of skin tissue.

Studies have indicated that DNFB-induced atopic dermatitis results in a notable upregulation expression levels of inflammatory factors, including TNF-α [31], IL-6 [32], IL-1β [33], and IL-8 [34]and accelerating the occurrence of inflammation and hindering skin inflammatory healing, which may also lead to scar formation or hypertrophic scarring [35, 36].The pathogenesis of AD is complex and is mostly associated with the disruption of skin barrier and the release of various inflammatory mediators by mast cells, including interleukin-8 (IL-8), tumor necrosis factor-α (TNF-α), IL-1β, IL-6, and chemokines.These mediators further promote inflammatory responses by recruiting and

**Table 4** Determination of the viscosity of carbomer at different concentrations

| Formulation | Viscositya (cps) |
|---|---|
| 0.5% Carbomer 940 gel | 28,237 ± 981 |
| 1% Carbomer 940 gel | 43,417 ± 1193 |
| 2% Carbomer 940 gel | 53,483 ± 401 |

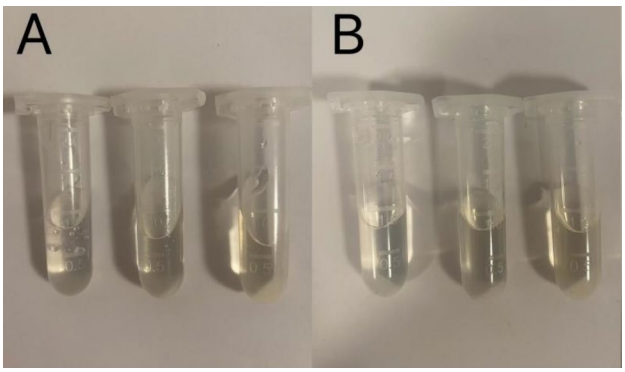


**Fig. 11** Appearance of 2% PL-CG under the high-speed centrifugation experiment (**A**); Appearance of 2% PL-CG under the alternating heat and cold experiment (**B**)

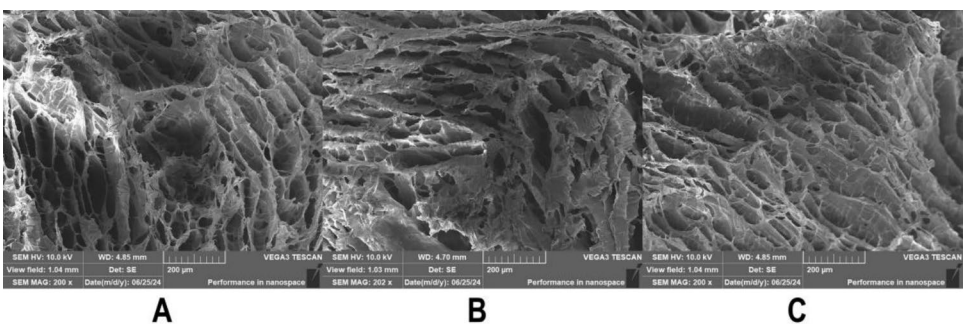


**Fig. 10** Microstructure of PL-CG at different concentrations. **A** 0.5%PL-CG; **B** 1%PL-CG; **C** 2%PL-CG

**Table 5** Stability test for PL-CG

| Stability test name | Color Change (None) | Stratification (None) | Other Changes (None) |
|---|---|---|---|
| High-speed Centrifugation Test | √ | √ | √ |
| Alternating Heat and Cold Experiment | √ | √ | √ |

activating immune cells. Among them, IL-1β is a cytokine released by keratinocytes after the epidermal barrier is disrupted. It can activate dendritic cells to secrete cytokines, leading to an imbalance in Th cell differentiation and subsequent skin barrier damage [37]. Monocyte chemoattractant protein-1 (MCP-1) plays a positive regulatory role in allergic diseases. It participates in early inflammatory responses and can promote the release of a large number of inflammatory mediators, predominantly histamine [38]. TNF-α is a pleiotropic pro-inflammatory factor that can induce lymphocytes to release a large amount of cytokines and significantly promote the release of thymic stromal lymphopoietin, thereby disrupting epidermal morphology and barrier function [39]. The experimental results demonstrate that PL-CG can significantly suppress the mRNA expression of the inflammatory cytokines IL-1β, IL-6, IL-8, and TNF-α (Fig. 9A–D), thereby reducing the occurrence of inflammation and promoting skin inflammatory healing, as well as reducing the formation of scar tissue.Significantly, during the course of treatment, we observed that mice in the dexamethasone-treated group exhibited polyuria, with their urine appearing yellow and having a strong odor, which may be related to adverse reactions following hormone administration. However, this phenomenon was not observed in any of the three concentrations of 0.5%PL-CG, 1%PL-CG, 2%PL-CG groups.

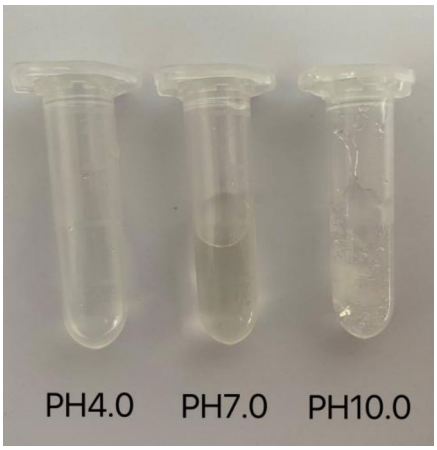


**Fig. 12** Appearance of Carbomer under Different pH Values

Patients with atopic dermatitis may find that inadequate itch control can significantly impact their quality of life, leading to poor sleep and potentially triggering depressive symptoms [40]. Therefore, finding medications capable of treating itch associated with atopic dermatitis has become crucial. Hydrogels, including Carbomer 940, have been widely used for topical and transdermal drug delivery due to their effective utilization in a wide range of applications [41]. Carbomer 940 is a high-quality, biodegradable hydrogel with no reported side effects [42].It has been shown to be non-toxic [43] and has been extensively used as a drug delivery medium [44, 45]. In this study, the

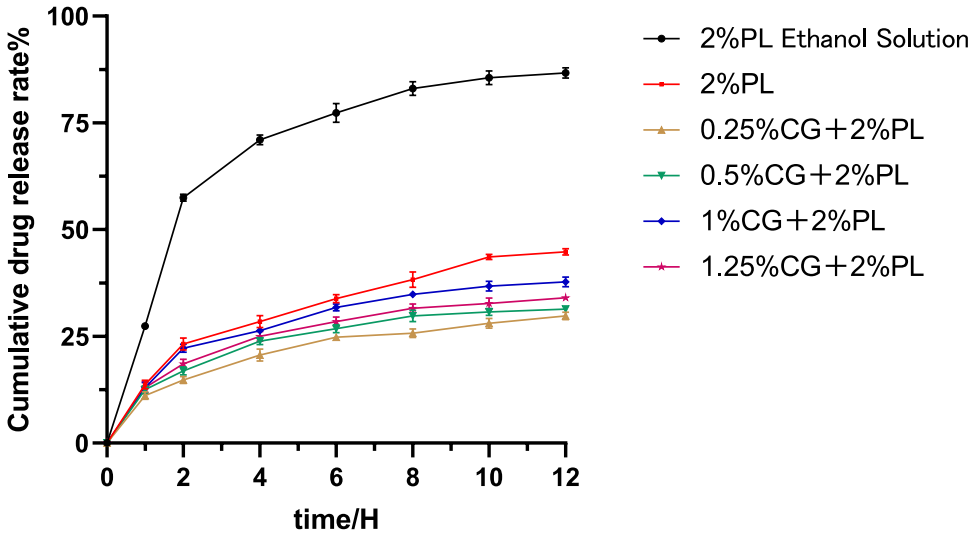


**Fig. 13** In vitro release curves of 2% PL solution with varying CG contents

**Table 6** Fitting Results of Release Kinetic Parameters for PL-CG

| The addition amount of Carbomer 940/% | Zero-order release $R^2$ | First-order release $R^2$ | Higuchim $R^2$ | Weibull $R^2$ |
|---|---|---|---|---|
| 0 | 0.73254 | 0.97728 | 0.84676 | 0.98568 |
| 0.25 | 0.9356 | 0.94559 | 0.98223 | 0.99588 |
| 0.5 | 0.89694 | 0.95550 | 0.96462 | 0.99647 |
| 1 | 0.90037 | 0.97369 | 0.97144 | 0.99141 |
| 1.25 | 0.90576 | 0.97346 | 0.97341 | 0.99683 |

characteristics of Carbomer 940 were leveraged to prolong the skin residence time of the drug. The scratching frequency of mice in the DXM group and the 0.5% PL-CG, 1% PL-CG, and 2% PL-CG group was significantly lower than that of the Control group (Fig. 7), indicating that PL-CG can effectively alleviate the pruritus symptoms in mice. In summary, PL-CG exhibits anti-inflammatory properties in dermatitis, effectively relieving skin itching without apparent toxic or side effects. However, the development of targeted therapies for atopic dermatitis is still in the early stages compared to other diseases [46].This study provides a foundational experimental basis for the potential therapeutic value of PL-CG as a targeted drug candidate for the future.

## Conclusions

The experimental outcomes manifest that PL-CG manifests outstanding capabilities in suppressing inflammatory responses, alleviating itching, diminishing inflammatory exudation on the skin surface, and ultimately expediting the healing of skin inflammation. Carbomer 940, which is a commonly employed drug delivery vehicle in clinical settings, when combined with PL in an effective manner, not only safeguards the activity of the drug but also extends its duration of efficacy. In contrast to conventional corticosteroid medications, PL-CG demonstrates diminished toxicity and fewer side effects. Moreover, PL, sourced from apple trees, can be extracted with simplicity and convenience, rendering the production cost of PL-CG relatively low. These discoveries furnish compelling justifications for the clinical promotion of PL-CG in the treatment of atopic dermatitis and present a novel substitute for traditional treatment modalities. Nevertheless, additional clinical investigations remain requisite to corroborate these findings.

**Acknowledgements** We are grateful to the Care and Use of Laboratory Animals Center of Guangdong Pharmaceutical University for providing excellent animal care, conducting rigorous observations, and generating detailed reports.All authors have read and agreed to the published version of the manuscript. All authors of this article agree that Professor Chen Weiqiang will be the main corresponding author. Ms. Yuan-ying Deng is the secondary corresponding author or co-corresponding author.

**Institutional review board statement** All animal procedures were carried out in accordance with the Guidelines for the Care and Use of Laboratory Animals of Guangdong Pharmaceutical University. The Animal Ethics Committee approved these procedures (NO. gdpulacspf2022277).

**Author contributions** Author Contributions: 1.Fulu Lv: Conceptualization, Data curation, Formal analysis, Investigation, Methodology, Resources, Writing—original draft. 2.Yanxia Chen: Data curation, Formal analysis, Investigation, Resources, Software, Writing—review & editing. 3.Haohui Xie: Data curation, Investigation. 4.Manzhi Gao:Formal analysis. 5.Ruohong He: Formal analysis and investigation. *Correspinding authors. 1.Weiqiang Chen: Writing-review and editing, Supervision, Project administration, Conceptualization, Methodology, Writing-review and editing, Resources, Funding acquisition. 2.WanYing Deng: Project administration, Supervision, funding acquisition. All authors have read and agreed to the published version of the manuscript. All authors of this article agree that Professor Chen Weiqiang will be the main corresponding author. Ms. Yuan-ying Deng is the secondary corresponding author or co-corresponding author.

**Funding** This research has been supported by grants from the New Generation of InformationTechnology of Guangdong Provincial Department of Education: (grant nos.2020ZDZX3026 belong to Weiqiang Chen)and the Guangdong Provincial Bureau of Traditional Chinese Medicine Project (Grant number 20241170 belong toWanYing Deng).

**Data availability** No datasets were generated or analysed during the current study.

## Declarations

**Conflict of interest** The authors declare no competing interests.

**Patient informed consent** Not applicable.

## References

1. Saha S, Barik D, Biswas D (2024) AMPs as host-directed immunomodulatory agents against skin infections caused by opportunistic bacterial pathogens. Antibiotics 13(5):439
2. Segre JA (2006) Epidermal barrier formation and recovery in skin disorders. J Clin Invest 116(5):1150–1158
3. Sacotte R, Silverberg JI (2018) Epidemiology of adult atopic dermatitis. Clin Dermatol 36(5):595–605
4. Maspero J, De Paula Motta N, Rubini J, Zhang G, Sanclemente JR, Amador M.H. El, Sayed A. Chan, Wai Ming RP, Dodiuk-Gad I, Hamadah S, Thevarajah C, Rincón-Perez E, Fedenko YW, Yew MBY, Tang CY, Chu K, Kulthanan OS, Kucuk A, Al-Hammadi L, Brignoli A, Tsankova S, El-Samad JE, Neves L.E (2023) Epidemiology of adult patients with atopic dermatitis in AWARE 1: a second international survey. World Allergy Organ J. 16(3):100724
5. Nutten S (2015) Atopic dermatitis: global epidemiology and risk factors. Ann Nutr Metab 66(Suppl. 1):8–16

6. Schneider S, Li L, Zink A (2021) The new era of biologics in atopic dermatitis: a review. Dermatol Pract Concept 11(4):e2021144
7. Zink AGS, Arents B, Fink-Wagner A, Seitz IA, Mensing U, Wettemann N, de Carlo G, Ring J (2019) Out-of-pocket costs for individuals with atopic eczema: a cross-sectional study in nine European countries. Acta Derm Venereol 99(3):263–267
8. Radhakrishnan J, Kennedy BE, Noftall EB, Giacomantonio CA, Rupasinghe HPV (2024) Recent advances in phytochemical-based topical applications for the management of eczema: a review. Int J Mol Sci 25(10):5375
9. Broeders JA, Ahmed Ali U, Fischer G (2016) Systematic review and meta-analysis of randomized clinical trials (RCTs) comparing topical calcineurin inhibitors with topical corticosteroids for atopic dermatitis: a 15-year experience. J Am Acad Dermatol 75(2):410-419.e3
10. Alsterholm M, Af Klinteberg M, Vrang S, Sigurdardottir G, Sandström Falk M, Shayesteh A (2025) Topical steroid withdrawal in atopic dermatitis: patient-reported characterization from a Swedish social media questionnaire. Acta Derm Venereol. 105:adv40187
11. Gosch C, Halbwirth H, Stich K (2010) Phloridzin: biosynthesis, distribution and physiological relevance in plants. Phytochemistry 71(8–9):838–843
12. Boots AW, Drent M, de Boer VC, Bast A, Haenen GR (2011) Quercetin reduces markers of oxidative stress and inflammation in sarcoidosis. Clin Nutr 30(4):506–512
13. Oliveira RA, Fierro IM (2018) New strategies for patenting biological medicines used in rheumatoid arthritis treatment. Expert Opin Ther Pat 28(8):635–646
14. Antika LD, Lee EJ, Kim YH, Kang MK, Park SH, Kim DY, Oh H, Choi YJ, Kang YH (2017) Dietary phlorizin enhances osteoblastogenic bone formation through enhancing β-catenin activity via GSK-3β inhibition in a model of senile osteoporosis. J Nutr Biochem 49:42–52
15. Ferreira KCB, Valle A, Paes CQ, Tavares GD, Pittella F (2021) Nanostructured lipid carriers for the formulation of topical anti-inflammatory nanomedicines based on natural substances. Pharmaceutics 13(9):1454
16. Picos-Salas MA, Leyva-López N, Bastidas-Bastidas PJ, Antunes-Ricardo M, Cabanillas-Bojórquez LA, Angulo-Escalante MA, Heredia JB, Gutiérrez-Grijalva EP (2024) Supercritical CO(2) extraction of naringenin from Mexican oregano (Lippia graveolens): its antioxidant capacity under simulated gastrointestinal digestion. Sci Rep 14(1):1146
17. Wang L, Wu X, Wan Q, Yang Y, Gao C (2024) Phloridzin reduces synovial hyperplasia and inflammation in rheumatoid arthritis rat by modulating mTOR pathway. Int Immunopharmacol 133:111727
18. Sharma K, Ramachandran V, Sharma A, Mohanasundaram T, Mageshkumar H (2024) Phloridzin's diabetic wound healing potential through DPP-4 enzyme inhibition: a review article. Curr Diabetes Rev. https://doi.org/10.2174/0115733998291941240416053855
19. Zhang X, Li L, Chen J, Hu M, Zhang Y, Zhang X, Lu Y (2023) Investigation of anti-depression effects and potential mechanisms of the ethyl acetate extract of Cynomorium songaricum Rupr. through the integration of in vivo experiments, LC-MS/MS chemical analysis, and a systems biology approach. Front Pharmacol 14:1239197
20. Chen H, Dong L, Chen X, Ding C, Hao M, Peng X, Zhang Y, Zhu H, Liu W (2022) Anti-aging effect of phlorizin on D-galactose-induced aging in mice through antioxidant and anti-inflammatory activity, prevention of apoptosis, and regulation of the gut microbiota. Exp Gerontol 163:111769
21. Guo Q, Li TF, Huang J, Li JC, Zhang ZC, Qu YL (2024) The protective role of phlorizin against lipopolysaccharide-induced acute orchitis in mice associated with changes in gut microbiota composition. Front Vet Sci 11:1340591
22. Beyer L, Kabatas AS, Mommert S, Stark H, Werfel T, Gutzmer R, Schaper-Gerhardt K (2022) Histamine Activates Human Eosinophils via H(2)R and H(4)R Predominantly in Atopic Dermatitis Patients. Int J Mol Sci 23(18):10294
23. Schaper-Gerhardt K, Rossbach K, Nikolouli E, Werfel T, Gutzmer R, Mommert S (2020) The role of the histamine H(4) receptor in atopic dermatitis and psoriasis. Br J Pharmacol 177(3):490–502
24. Alcain J, Infante Cruz ADP, Barrientos G, Vanzulli S, Salamone G, Vermeulen M (2022) Mechanisms of unconventional CD8 Tc2 lymphocyte induction in allergic contact dermatitis: Role of H(3)/H(4) histamine receptors. Front Immunol 13:999852
25. Jutel M, Akdis CA (2007) Histamine as an immune modulator in chronic inflammatory responses. Clin Exp Allergy 37(3):308–310
26. Desai P, Thurmond RL (2011) Histamine $H_4$ receptor activation enhances LPS-induced IL-6 production in mast cells via ERK and PI3K activation. Eur J Immunol 41(6):1764–1773
27. Zhang B, Alysandratos KD, Angelidou A, Asadi S, Sismanopoulos N, Delivanis DA, Weng Z, Miniati A, Vasiadi M, Katsarou-Katsari A, Miao B, Leeman SE, Kalogeromitros D, Theoharides TC (2011) Human mast cell degranulation and preformed TNF secretion require mitochondrial translocation to exocytosis sites: relevance to atopic dermatitis. J Allergy Clin Immunol 127(6):1522–31.e8
28. Goldberg MT, Han YP, Yan C, Shaw MC, Garner WL (2007) TNF-alpha suppresses alpha-smooth muscle actin expression in human dermal fibroblasts: an implication for abnormal wound healing. J Invest Dermatol 127(11):2645–2655
29. Hong YK, Chang YH, Lin YC, Chen B, Guevara BEK, Hsu CK (2023) Inflammation in wound healing and pathological scarring. Adv Wound Care 12(5):288–300
30. Sorg H, Tilkorn DJ, Hager S, Hauser J, Mirastschijski U (2017) Skin wound healing: an update on the current knowledge and concepts. Eur Surg Res 58(1–2):81–94
31. Yang X, Wang Z, Huang H, Luo G, Cong L, Yang J, Ye J (2024) Jianpi Yangxue Qufeng compound alleviates atopic dermatitis via TLR4/MyD88/NF-κB signaling pathway. Heliyon 10(1):e23278
32. Liang YH, Shu P, Li YL, Li M, Ye ZH, Chu S, Du ZY, Dong CZ, Meunier B, Chen HX (2023) GDU-952, a novel AhR agonist ameliorates skin barrier abnormalities and immune dysfunction in DNFB-induced atopic dermatitis in mice. Biochem Pharmacol 217:115835
33. Gao JF, Tang L, Luo F, Chen L, Zhang YY, Ding H (2023) Myricetin treatment has ameliorative effects in DNFB-induced atopic dermatitis mice under high-fat conditions. Toxicol Sci 191(2):308–320
34. Aye A, Song YJ, Jeon YD, Jin JS (2020) Xanthone suppresses allergic contact dermatitis in vitro and in vivo. Int Immunopharmacol 78:106061
35. Salgado RM, Alcántara L, Mendoza-Rodríguez CA, Cerbón M, Hidalgo-González C, Mercadillo P, Moreno LM, Alvarez-Jiménez R, Krötzsch E (2012) Post-burn hypertrophic scars are characterized by high levels of IL-1β mRNA and protein and TNF-α type I receptors. Burns 38(5):668–676
36. Wang ZC, Zhao WY, Cao Y, Liu YQ, Sun Q, Shi P, Cai JQ, Shen XZ, Tan WQ (2020) The roles of inflammation in keloid and hypertrophic scars. Front Immunol 11:603187
37. Barker JN, Jones ML, Mitra RS, Crockett-Torabe E, Fantone JC, Kunkel SL, Warren JS, Dixit VM, Nickoloff BJ (1991) Modulation of keratinocyte-derived interleukin-8 which is chemotactic for neutrophils and T lymphocytes. Am J Pathol 139(4):869–876

38. González-de-Olano D, Álvarez-Twose I (2018) Mast cells as key players in allergy and inflammation. J Investig Allergol Clin Immunol 28(6):365–378
39. Kim J, Kim BE, Leung DYM (2019) Pathophysiology of atopic dermatitis: clinical implications. Allergy Asthma Proc 40(2):84–92
40. Andersen L, Nyeland ME, Nyberg F (2020) Higher self-reported severity of atopic dermatitis in adults is associated with poorer self-reported health-related quality of life in France, Germany, the UK and the U.S.A. Br J Dermatol 182(5):1176–1183
41. Wang Z, Xue Y, Zhu Z, Hu Y, Zeng Q, Wu Y, Wang Y, Shen C, Jiang C, Liu L, Zhu H, Liu Q (2022) Quantitative structure-activity relationship of enhancers of licochalcone A and glabridin release and permeation enhancement from carbomer hydrogel. Pharmaceutics 14(2):262
42. Wang D, Jin J, Zhang C, Ruan C, Qin Y, Li D, Guan M, Lei P (2024) Carbomer hydrogel composed of Cu(2)O and hematoporphyrin monomethyl ether promotes the healing of infected wounds. ACS Omega 9(4):4974–4985
43. Ojha C, Sharma P, Jain V (2024) Design, optimization, and evaluation of topical gel of Cardiospermum halicacabum and Ricinus communis L. leaves extract for the treatment of rheumatoid arthritis. J Biomater Sci Polym Ed 35(10):1584–1605
44. Jing G, Suhail M, Lu Y, Long B, Wu Y, Lu J, Ge J, Iqbal MZ, Kong X (2024) Engineering titanium-hydroxyapatite nanocomposite hydrogels for enhanced antibacterial and wound healing efficacy. ACS Biomater Sci Eng. https://doi.org/10.1021/acsbiomaterials.4c00277
45. Li X, Bai L, Zhang X, Fang Q, Chen G, Xu G (2024) Application of Bletilla striata polysaccharide hydrogel for wound healing among in diabetes. Colloids Surf B Biointerfaces 241:114033
46. Sroka-Tomaszewska J, Trzeciak M (2021) Molecular mechanisms of atopic dermatitis pathogenesis. Int J Mol Sci 22(8):4130